Grant Agreement No. 783169
U-Geohaz – "Geohazard impact assessment for urban areas"

Deliverable D4.10: Rainfall thresholds for the Canary Islands

A deliverable of WP 4 (Activity 4.5): Rainfall thresholds for the possible initiation of rock falls

Due date of deliverable: 30/06/2019
Actual submission date: 23/07/2019

Lead contractor for this deliverable: IRPI

Dissemination Level		
PU	Public	X
PP	Restricted to other programme participants (including the Commission Services)	
RE	Restricted to a group specified by the Consortium (including the Commission Services)	
CO	Confidential, only for members of the Consortium (including the Commission Services)	
TN	Technical Note, not a deliverable, only internal for members of the Consortium	

European Union
Civil Protection and
Humanitarian Aid

Table of Content

EXECUTIVE SUMMARY

The document, which represents the fourth deliverable of WP4 “Tools and methods to support Early Warning System for Rock falls”, describes the actions performed in the Activity 4.5 “Rainfall thresholds for the possible initiation of rock falls”. The main goal of this activity is the definition of empirical rainfall thresholds for the possible initiation of rock falls in the Canary Islands.

The report describes the empirical cumulated event rainfall – rainfall duration (*ED*) thresholds for the Gran Canaria and Tenerife test sites. For the purpose, a tool for the objective and reproducible reconstruction of rainfall events and of rainfall conditions responsible for rock falls is used. A frequentist statistical method is adopted to define *ED* thresholds for different non-exceedance probabilities.

REFERENCE DOCUMENTS

N°	**Title**
RD1	DoW Part B

CONTRIBUTORS

Contributor(s)	Company	Contributor(s)	Company
Silvia Peruccacci	CNR-IRPI	Roberto Sarro	IGME
Stefano Luigi Gariano	CNR-IRPI	Rosa Maria Mateos	IGME
Maria Teresa Brunetti	CNR-IRPI	Gerardo Herrera	IGME
Massimo Melillo	CNR-IRPI	Marta Bejar	IGME
Paola Reichenbach	CNR-IRPI	Miguel Tomé	DGPCE
Ivan Marchesini	CNR-IRPI	Lucrecia Alguacil	DGPCE
Mauro Rossi	CNR-IRPI	Jorge Naranjo	CDCP
		Ada Martín	CDCP

REVIEW: CORE TEAM

Reviewed by	Company	Date	Signature
Oriol Monserrat	CTTC	06/07/2019	

1 INTRODUCTION

Rainfall is a recognized trigger of landslides, and investigators have long attempted to determine the amount of precipitation needed to trigger slope failures. Landslides triggered by rainfall are caused by the build-up of water pressure into the ground (Campbell, 1975; Wilson, 1989). Groundwater conditions responsible for slope failures are related to rainfall through infiltration, soil characteristics, antecedent moisture content, and rainfall history (Wieczorek, 1996).

Worldwide, rainfall-induced landslides are recurrent phenomena that cause societal and economic damage. Thus, assessing the rainfall conditions responsible for landslides is important and may contribute to reducing risk.

At regional and global scales, empirical approaches to forecast the occurrence of rainfall-induced landslides rely upon the definition of rainfall thresholds, i.e. the rainfall conditions that when reached or exceeded are likely to result in single or multiple landslides. Several authors have proposed different methods to compute rainfall thresholds through the statistical analysis of empirical distributions of rainfall conditions that have presumably resulted in landslides including cumulated event rainfall vs. rainfall duration or mean rainfall intensity vs. rainfall duration (e.g., Aleotti, 2004; Guzzetti et al., 2007, 2008; Brunetti et al., 2010; Berti et al., 2012; Giannecchini et al., 2012; Martelloni et al., 2012; Peruccacci et al., 2012; Staley et al., 2013; Segoni et al., 2014; Rosi et al., 2016; Peruccacci et al., 2017).

Rainfall thresholds are affected by uncertainties that limit their use in operational warning systems. A source of uncertainty lies in the characterization of the rainfall events responsible for landslides. Objective criteria for the definition of rainfall events are lacking. To overcome the problem, Melillo et al. (2018) have proposed an algorithm that reconstructs rainfall events, identifies the rainfall conditions that have resulted in landslides, and calculates probabilistic cumulated event rainfall- rainfall duration (*ED*) thresholds and their associated uncertainties.

The main goal of WP4 is to tailor tools and methods to generate information useful to support early warning systems for rock falls. An important element to mitigate landslide hazard and risk is the definition of an operational landslide warning system based on the comparison between rainfall measurements and forecasts and rainfall thresholds, aiming at evaluating the possible occurrence of landslides.

The present document is an update of the previous deliverable “Preliminary rainfall thresholds for the Canary Islands” (D4.9) released in September 2018.

The document is organized as follows. After a description of the general settings of the Canary Islands and of the U-Geohaz two test sites (Section 2), we describe the catalogue of rainfall events that have caused rock falls in Tenerife Island and along the GC-200 road (Gran Canaria), and the sources and method used for its compilation (Section 3). Next, we describe the CTRL Tool (CTRL-T) used to determine *ED* rainfall thresholds (Section 4). Finally, we exploit the two catalogues to define empirical rainfall thresholds for possible rock fall occurrence in GC-200 and Tenerife test sites (Section 5).

2 TEST SITE DESCRIPTIONS

The Canary Islands is an archipelago of seven major volcanic islands constituting the outermost Spanish region in the Atlantic Ocean on the continental slope and rise of western Africa (Figure 1). The islands lie 2000 km east of the Mid-Atlantic Ridge and 150 km west of Morocco. From east to west, the islands are Lanzarote, Fuerteventura, Gran Canaria, Tenerife, La Gomera, La Palma, and El Hierro. The eruptive history of the islands extend from 40 Ma until the present (El Hierro), making them one of the major volcanic oceanic island groups of the world. Most of the historical eruptions in the Canary Islands have been short-lived basaltic or strombolian eruptions, which have caused pyroclastic cones of different size and lava flows of different extent and height.

The steep topography and the geological complexity of the archipelago influence the activation of intense slope dynamics and many slope failures occur along the slopes. Rock falls are the most frequent and damaging landslide type in the Canary Islands, causing damages on built-up areas and communication networks. To define empirical rainfall thresholds for the possible initiation of rock falls, two test sites were selected following the emergency services priorities. The first site is located in the northwestern part of Gran Canaria Island, along the GC-200 road between the localities of Agaete and Aldea. The second site is represented by the entire Tenerife Island.

Figure 1. The Canary island archipelago. Empirical rainfall thresholds for the possible initiation of rock falls were defined in two test sites (red boxes).

2.1 GC-200 road (Gran Canaria Island)

Gran Canaria is the third island in size of the Canary Islands, with an area of 1560 km^2 and a maximum altitude of 1956 m. The origin of the island can be dated about 15 million years ago with the first submarine building stages of the Gran Canaria Volcano. Figure 2 shows a simplified geological map of the island with the main lithological units. The main stages of evolution of Gran Canaria are: i) the shield stage, including a basaltic shield volcano; ii) the vertical caldera collapse, giving place to the Tejeda-Fataga complex, with a salic post-caldera resurgence; and iii) a rejuvenated stage, including the Roque Nublo stratovolcano and the post- Roque Nublo volcanism (late eruptive phase) which created a composite monogenetic volcanic field.

Additionally, massive flank failures are mapped (see gravitational failures) giving place to chaotic deposits that cover large areas.

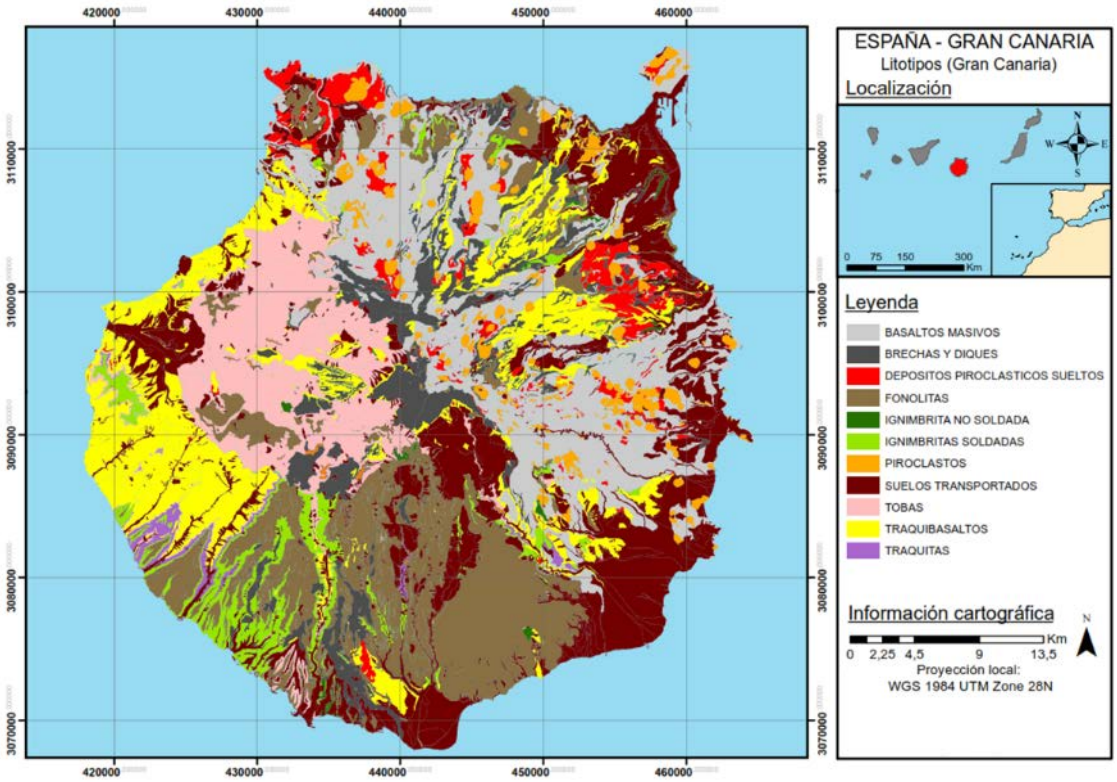

Figure 2. Gran Canaria Island. Simplified geological map.

Regarding climatological conditions, Gran Canaria is located in a transitional zone between temperate and tropical conditions. The conical morphology of Gran Canaria retains the humidity of the predominant north/northeast trade winds of the subtropical Azores anticyclone on the north side of the island. As a result, the northern flanks are humid and vegetation is vigorous, while the south is very dry and the conditions are very arid and desert-like. Rainfall increases with altitude, ranging between less than 200 mm/yr at the coast and over a wide area in southern Gran Canaria, and more than 1400 mm/yr in the higher peaks of the central part of the island. The climate in the test-site area is very dry, with an annual average precipitation of 300 mm and the annual average temperature of 20.6º. The maximum precipitation takes place during the autumn and winter months, with December the rainiest month. Heavy storms are frequent, associated with intense rainfall and strong winds, with events measuring of up to 75 mm in 24 hours.

The GC-200 road test site (Figure 3) is located in the western part of the island, between the localities of Agaete and Aldea, representing the main transportation corridor between the two localities. The road has a length of 34 km, with a very tortuous path following the coastline, a very step coast with the highest cliffs in Europe (Risco Faneque, 1027 m a.s.l.). The road is a strategic infrastructure for the transportation of the tomato production, cultivated in numerous greenhouses in Aldea. Moreover, the road an important touristic attraction due to the spectacular landscape

views. The road has heavy traffic estimated on average with 1500 vehicles per day, with a greater number of vehicles during the period from October to May. The geology of the test-site area is in the domain of the basaltic shield stage, Middle Miocene in age. Along the road, an alternate of alkaline basaltic deposits (hard rocks) and pyroclastic flows can be observed. Both materials can be source areas for rock falls blocks. In some parts, gravitational deposits also outcrop and some boulders frequently occupy the road.

Figure 3. Gran Canaria Island. Panoramic view of the GC-200 road.

2.2 Tenerife Island

Tenerife is located in the central part of the Archipelago, between 27º 59' 59'' N and 28º 35' 15'' N and 16º 50' 27'' W and 16º 55' 40'' W. It is the largest island with a surface of 2057 km^2 and the most populated. Its highest point, Mount Teide, with an elevation of 3718 meters, is the highest point of Spain and the third largest volcano in the world considering the base at the bottom of the sea.

From the geological point of view, all Canary Islands are located inside the Africa Plate, in the transitional zone between the Continental Crust and the Oceanic Crust, characterized by the volcanic origin that is still active. The tectonic lines are responsible for the island shape– a triangle-, with a clear predominance of NE-SW and NW-SE directions during the main building phases. The principal structures in the Tenerife make the central highlands, with the Teide–Pico Viejo complex and the Las Cañadas areas, the most prominent area with a surface of 130 km^2. Las Cañadas caldera was formed by a vertical collapses produced after intense explosive volcanic activity. The area is partially occupied by the Teide-Pico Viejo strato-volcano and by the volcanic materials derived by different eruptions. The location of Tenerife Island in the middle of the archipelago explains the impressive relief, the large variations of volcanic rocks types and the

different volcanic structures and landforms. The steep orography (Figure 4) of the island and the climate variety have resulted in a diversity of landscapes and geographical formations. The Teide National Park is characterized by extensive pine forests juxtaposed against the volcanic landscape at the summit of Teide and Malpaís de Güímar, to the Acantilados de Los Gigantes (Cliffs of the Giants) with its vertical precipices.

Figure 4. Tenerife Island. Panoramic view of the Anaga range in the northern part of the island.

The trade-winds affect the island during the main part of the year, from May to September. The trade-winds present a double layer, the lower being wet and temperate blowing over the ocean from N-NE direction and the upper being warm and very dry blowing from W-NW direction. This layered structure produces a stable situation in the atmosphere. The landforms act as interference with the regional atmosphere circulation producing a wide variety of local climates. North areas are exposed to trade-winds and Atlantic winds, producing the south slopes drier than the north ones; in the northern slopes the presence of the temperature inversion produces a sea cloud, between 500 m to 1500 m high, setting unusual wet conditions and supporting an extra amount of water by fog rain. Several experiments provided evidence for supplies of fog rain four times higher than normal rain. During winter, the Atlantic low pressure causes rainy weather and even snow fall above 1500 meters.

3 RAINFALL AND LANDSLIDE DATA

In the test areas, rainfall measurements were obtained from national and regional rain gauge networks. For the selection of the rain gauges, the availability of time series, the data quality and the location of the rain gauge were taken into account, given that these features are crucial to characterize the spatio-temporal variation of the precipitations.

For the Tenerife island test site, we have used the rain gauge network provided by the Spanish National Meteorological Service (AEMET). Additional rain gauges provided by regional institutions as Agrocabildo- Servicio Técnico de Agricultura y Desarrollo Rural, and validated by AEMET were included to increase the rainfall information used in this update. The analysis was performed using both daily and hourly data from the AEMET network, which were available for the periods 2010-2017 and 2000-2016, respectively. As a result, a long time series of rainfall data was obtained, which is fundamental to calculate reliable thresholds. The two networks in the Tenerife test site are composed by 34 rain gauges recording hourly data and 66 rain gauges recording daily data, distributed on the island (Figure 5).

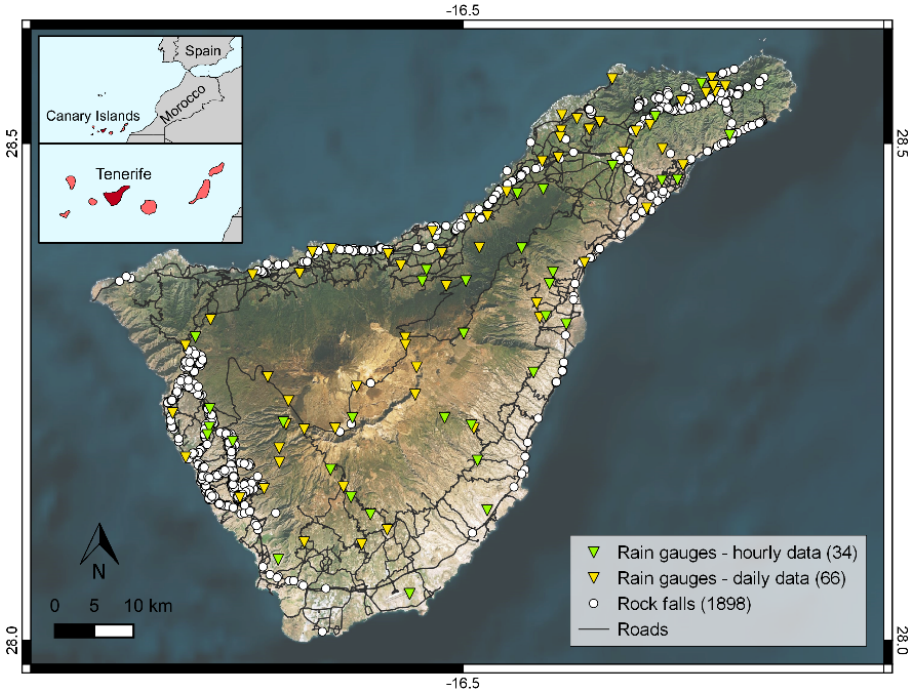

Figure 5. Tenerife test site. Location of the rain gauges with hourly (green triangles) and daily (yellow triangles) rainfall measurements, and of rock falls included in the catalogue (white dots).

The daily and hourly rainfall measurements were stored in a txt file, which contains information on the rain gauge code, rain gauge name, date, geographical coordinates, elevation, and daily or hourly measurements. The daily rainfall is referred to the time period between 07:00 UTC of the previous day to 07:00 UTC of the day of measurement. This information was stored in a worksheet for the calculation of rainfall thresholds.

As concern the rock fall data, we used the inventory of the Tenerife Island prepared by the Canarian Civil Protection Authorities that registered accurately the location of each rock fall impact along the Tenerife roads. In the period from January 2010 to November 2017, 1898 rock falls were detected. From the rock fall inventory, we have developed a worksheet to store all data. For each event, the catalogue contains the following information: event code, localization, geographic accuracy, and temporal information of the failure (day, month, year, time, date, temporal accuracy).

To reduce the use of wrong information (i.e., incorrectly dated landslides) in the definition of the thresholds, we discarded all rainfall conditions having a delay longer than 48 hours between the rainfall ending time and the landslide occurrence.

In the Tenerife test site, between 2010 and 2016, 245 rock falls were selected for the analysis with daily rainfall (red dots in Figure 6) and 381 with hourly rainfall (red dots in Figures 7). Regarding the monthly distribution, in the Tenerife test site, almost all events were recorded between October and April, with a maximum in November. No landslides were recorded in July (Figure 8a). The yearly distribution of these events exhibits a peak in 2014 (90 records with hourly data, 66 with daily data), 2015 and 2013 (Figure 8b). The 245 daily rainfall conditions associated to the rock falls have durations ranging from 1 to 15 days and mean value of 2 days. The values of cumulated rainfall range from 15.4 to 235 mm, with an average of 71.5 mm. The average distance between the landslides and the representative rain gauges is 2.2 km, with a maximum distance of 5 km.

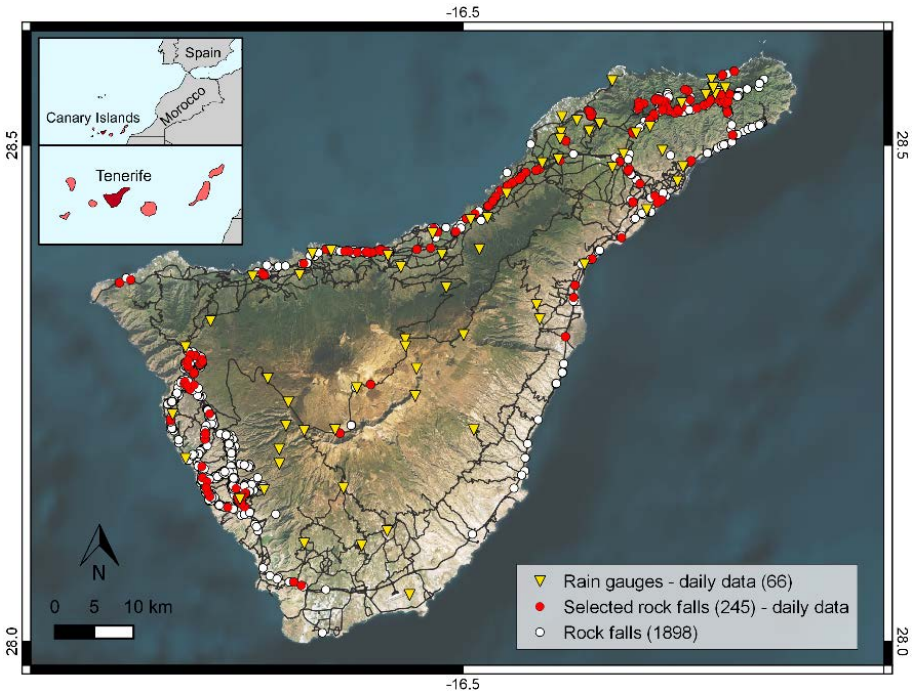

Figure 6. Tenerife test site. Location of the rain gauges with daily rainfall measurements (yellow triangles), and of rock falls: white dots show all the rock falls in the catalogue; red dots the events selected to calculate the thresholds.

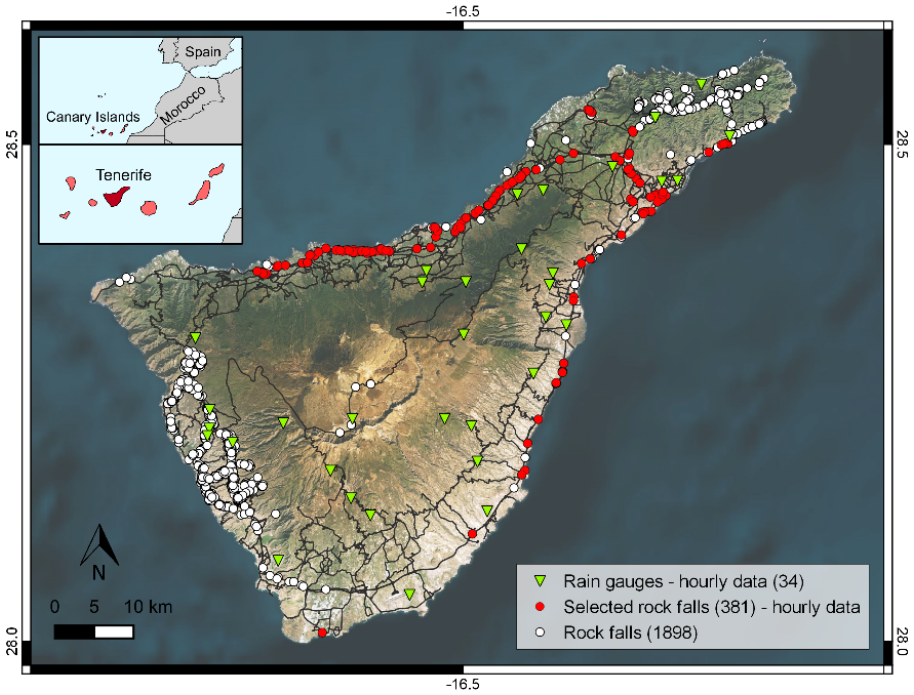

Figure 7. Tenerife test site. Location of the rain gauges with hourly rainfall measurements (green triangles), and of rock falls: white dots show all the rock falls in the catalogue; red dots the events selected to calculate the thresholds.

The 381 hourly rainfall conditions associated to the rock falls have durations ranging from 2 to 712 hours and mean value of 111 hours. The values of cumulated rainfall range from 10.6 to 434.0 mm, with an average of 105.6 mm. The average distance between the landslides and the representative rain gauges is 6.7 km, with a maximum distance of 14.9 km. More details are reported in Table 1.

In the GC-200 test site (Gran Canaria island), daily rainfall data from the Consejo Insular de Aguas de Gran Canaria (CIAGC) regional rain gauge network (13 stations) and from AEMET national network (92 stations, among which 7 are close to the study area) were used for the analysis. Moreover, hourly rainfall data provided by AEMET national network (23 stations among which 4 are close to the study area) were used (Figure 9).

Rainfall data contains daily rainfall measurements collected in the period between January 2010 and December 2017 and hourly rainfall measurements collected in the period between January 2010 and December 2017. Following the same methodology applied in the Tenerife test site, for each rain gauge, data are stored in a worksheet, where the header contains information on rain gauge name, code, geographical coordinates, elevation and the daily rainfall in mm.

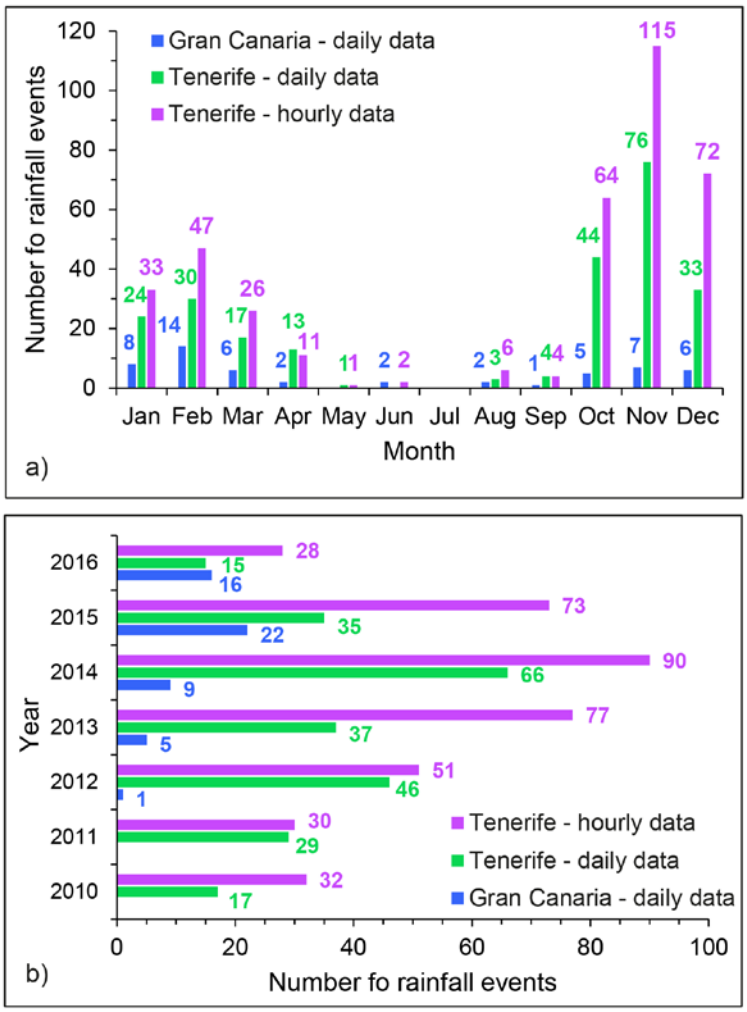

Figure 8. Monthly (a) and annual (b) distributions of the rainfall events reconstructed for the two test sites.

We have recorded the information and observations carried out by the Canarian Civil Protecion Authorities about rock fall events occurred from January 2010 to March 2016, along the GC-200 road. A total of 8174 rock fall events were documented and a digital inventory was prepared defining accurately the location of each impact along the road using orthophotos available for the region. The information for each event includes the kilometre point, number of events, date, boulder size, and was organized in a worksheet. This worksheet contains the following information for each event: event code, localization, geographic accuracy, and temporal information of the failure (day, month, year, time, date, temporal accuracy). We used only 535 rock fall events characterized by medium to large size, excluding small and very small rock falls, but only 53 rock falls were selected for the analysis with daily data (red dots in Figure 10) and 29 with hourly data (red dots in Figure 11). In particular, for the analysis with daily data, only the CIAGC network was considered, given its wider coverage of rain gauges in the study area; the AEMET network having only 7 stations close to the study area (yellow triangles in Figure 8).

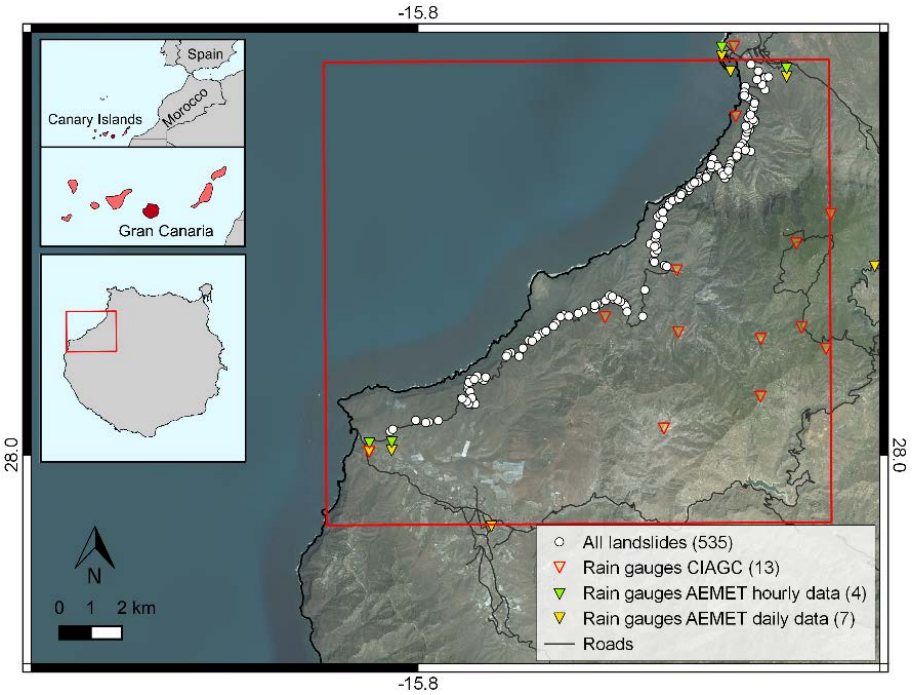

Figure 9. GC-200 test site, Gran Canaria island. Location of the rain gauges (triangles) and rock falls: white circles show all the rock falls in the catalogue; red circles the events selected to calculate the thresholds.

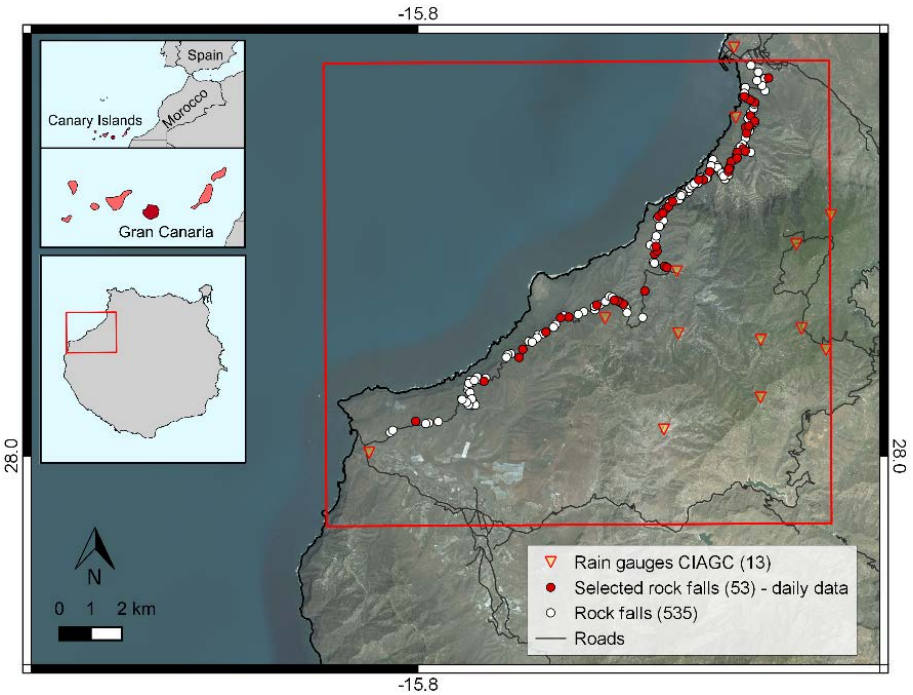

Figure 10. GC-200 test site, Gran Canaria island. Location of the rain gauges (triangles) and rock falls: white dots show all the rock falls in the catalogue; red dots are the events selected to calculate the thresholds.

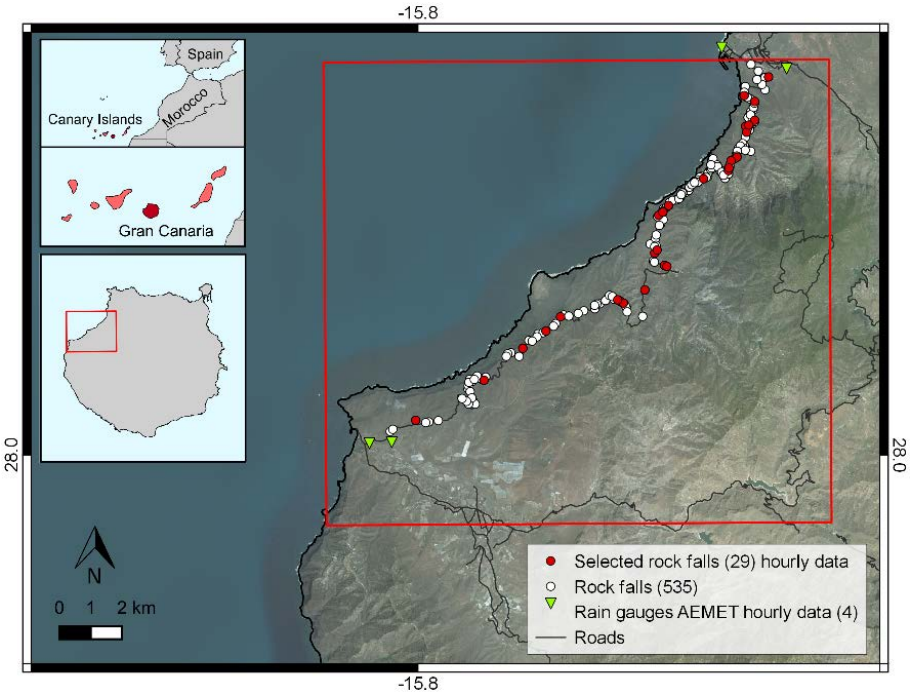

Figure 91. GC-200 test site, Gran Canaria island. Location of the rain gauges (green triangles) and rock falls: white dots show all the rock falls in the catalogue; red dots the events selected to calculate the thresholds.

Moreover, during the analysis, daily data from AEMET network were considered not representative for the triggering of the rock falls, because of the spatial location of the stations and the rainfall measurements. Moreover, the low number of selected rock falls in the analysis with hourly data is due to the scarce coverage of rain gauges in the study area.

The 53 events registered for the Gran Canaria test site (Figure 10) occurred between 2012 and 2016, most. of them in 2015 (22) and 2016 (16). Almost all the landslides were recorded in the semester October-March, with a peak in February (14 occurrences). Only 7 landslides occurred in the period April-September (Figure 8a). The 53 daily rainfall conditions responsible for the rock fall occurrences have durations in the range $1 \leq D \leq 11$ days (with an average value of 4 days) and cumulated rainfall in the range $16.5 \leq E \leq 219.9$ mm (average value 51.6 mm). All the conditions were recorded in rain gauges located at a maximum distance from the failures of 5.7 km, with a mean value of 2.8 km. More details are reported in Table 1.

Table 1. Minimum, mean, and maximum values of distance from rain gauge, duration and cumulated event rainfall of the rainfall events reconstructed for the two test sites.

		Rain gauge distance (km)	Duration *D* (h - d)	Cumulated event rainfall *E* (mm)
Gran Canaria test site (daily rainfall data)	Min	0.3	1 d	16.5
	Mean	2.8	4 d	51.6
	Max	5.7	11 d	219.9
Gran Canaria test site (hourly rainfall data)	Min	0.9	5 h	13.4
	Mean	10.0	68 h	71.2
	Max	14.8	288 h	266.6
Tenerife test site (daily rainfall data)	Min	0.2	1 d	15.4
	Mean	2.2	2 d	71.5
	Max	5.0	15 d	235.0
Tenerife test site (hourly rainfall data)	Min	0.3	2 h	10.6
	Mean	6.7	111 h	105.6
	Max	14.9	712 h	434.0

4 METHODS

Empirical rainfall thresholds are affected by several uncertainties, including: (i) the availability and quality of the rainfall measurements and of the landslide information; (ii) the characterization of the rainfall event responsible for the landslides; (iii) the heuristic or statistical methods used to determine the thresholds. Standards for measuring landslide-triggering rainfall conditions are still lacking or insufficiently formalized in literature and how the rainfall responsible for the landslide occurrence is calculated is rarely reported. Moreover, the majority of empirical rainfall thresholds available in the literature are calculated using subjective and scarcely repeatable methods.

We maintain that the quantitative identification of the landslide-triggering rainfall and the definition of reliable thresholds are fundamental steps towards a well-founded landslide prediction (Peruccacci et al., 2017; Melillo et al., 2018). The use of a standardized and automatized procedure for the reconstruction of the rainfall conditions responsible for failures and for threshold calculation is necessary for enhancing the objectivity and reproducibility of the thresholds, especially for thresholds to be used in landslide early warning systems. For the purpose, the algorithm CTRL-T proposed by Melillo et al. (2018) was exploited to calculate cumulated event rainfall- rainfall duration (*ED*) thresholds for the Canary Islands.

CTRL-T exploits continuous rainfall measurements, and landslide information, to (1) reconstruct rainfall events; (2) select automatically the representative rain gauges; (3) identify multiple rainfall conditions responsible for the failure in terms of *D* and *E*; (4) attribute a probability to each rainfall condition; and (5) calculate probabilistic rainfall thresholds and their associated uncertainties.

Figure 12 illustrates the logical framework of CTRL-T. The input data is composed by: (i) setting parameters of the rainfall events, (ii) rainfall data, (iii) rain gauge locations, (iv) landslide locations, and (v) landslide occurrence times. The algorithm is divided into three main logical blocks. The “BLOCK 1” executes the reconstruction of the rainfall events (RE). The “BLOCK 2” selects the rainfall events that have resulted in landslides and determines the rainfall duration, D_L, and the cumulated event rainfall, E_L, responsible for the landslides. The “BLOCK 3” calculates rainfall thresholds at different non-exceedance probabilities.

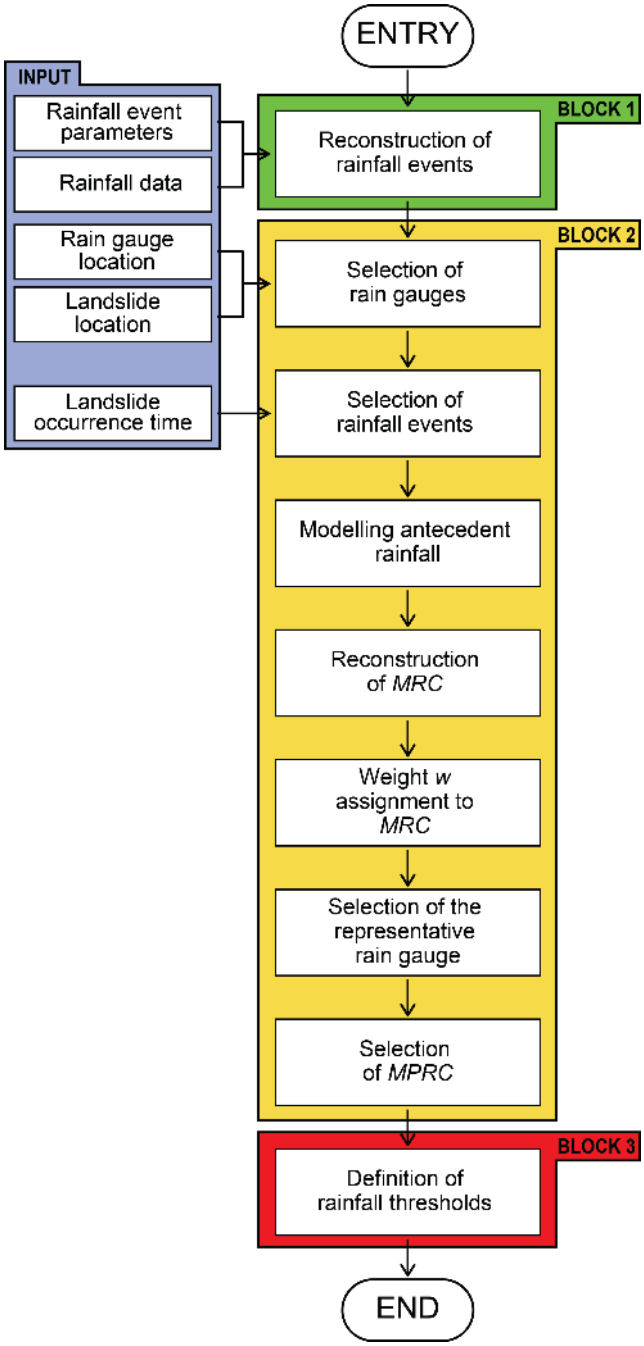

Figure 12. Logical framework of the algorithm in CTRL-T.

First, CTRL-T reconstructs individual rainfall events from a record of rainfall measurements. This is performed in five successive steps, including a pre-processing step. Figure 13 portrays the logical framework of “BLOCK 1”.

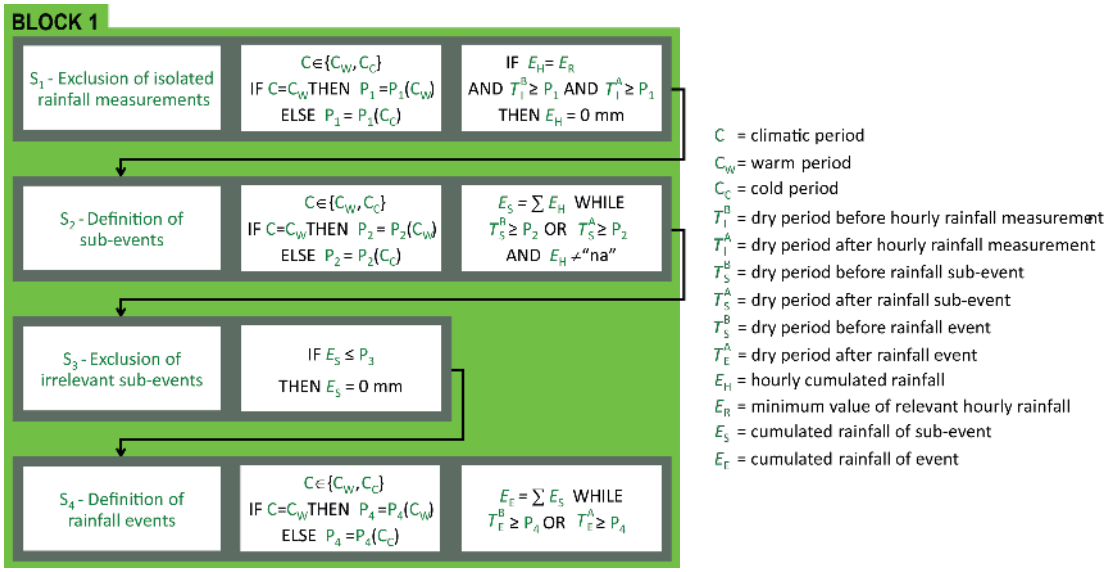

Figure 13. Logical framework of "BLOCK 1".

Step 0: Pre-processing of rainfall data

The tool works on a continuous (for the sake of the discussion, hourly) record of rainfall measurements obtained from a single rain gauge in a period. Records of rainfall measurements are typically discontinuous (incomplete), with individual or multiple rainfall measurements missing in the record due to technical and operational problems. The gaps in the record can cover periods ranging from a minimum of one hour to several days or weeks, and are typically marked by specific "tags" in the record, with different tags used to describe different types of technical and operational problems. Occasionally, tags are missing in the rainfall record, and it is difficult – or impossible – to single out measurements gaps in the record. The algorithm checks the continuity of the record and detects the gaps. More specifically, the algorithm searches the rainfall record for tagged and untagged missing measurements, and replaces them with the "na" tag (measurement not available).

In addition, a rainfall record may contain hourly rainfall measurements E_H that are lower than the instrumental sensitivity of a rain gauge (e.g., G_S = 0.2 mm), $E_H < G_S$. These hourly measurements are considered noise in the rainfall record, and the algorithm sets the measurements to E_H = 0.0 mm. Note that E_H = "na" is different from E_H = 0.0 mm. When E_H = "na" the rainfall information is missing in the record, whereas when E_H = 0.0 mm the rainfall information is available in the record and it is considered noise. Figure 14a shows a prototype example of a corrected rainfall record.

Step 1: Detection and exclusion of isolated rainfall measurements

The algorithm starts by searching for isolated hourly rainfall measurements in the corrected rainfall record (S_1 in Figure 13). An isolated rainfall measurement is defined as an hourly measurement separated from the immediately preceding and the immediately following rainfall measurements by dry periods (T_I^B before, and T_I^A after) that exceed a given length P_1. The length of the dry period (P_1) depends on the seasonal or the local climatic conditions C i.e., $P_1 = P_1(C)$.

In the Mediterranean region two seasonal periods can be identified for landslide initiation: (i) a "warm" spring-summer period C_W, and (ii) a "cold" autumn-winter period C_C. For the C_W warm period the dry interval separating isolated rainfall measurements is P_1 = 3 hours, and for the C_C cold period the dry interval is P_1 = 6 hours (Table 2). Once the isolated rainfall measurements are identified, their individual relevance for the reconstruction of the rainfall conditions responsible for possible landslide occurrence is evaluated. We consider relevant the isolated hourly rainfall measurements that exceed a minimum value E_R (e.g., E_R = 0.2 mm), $E_H > E_R$, and irrelevant the measurements with $E_H = E_R$. The later measurements, shown by red bars in Figure 14b, contribute a negligible (irrelevant) amount of rain to the rainfall event (e.g., due to the presence of fog and/or humidity in the air). For the purpose of the analysis, the algorithm sets the isolated, irrelevant measurements to E_H = 0.0 mm.

Step 2: Identification of rainfall sub-events

The algorithm proceeds by searching for individual rainfall sub-events (S_2 in Figure 13), where a rainfall sub-event is a period of continuous rainfall separated from the immediately preceding and the immediately following sub-events by dry periods with no rain. As before, the length P_2 of the dry period may vary, depending on the seasonal and the climatic conditions, $P_2 = P_2(C)$. The separation is justified by the observation that the meteorological conditions and the rainfall characteristics in the two climatic periods are different. In the C_W warm period, rainfall is primarily brought to the study area by local convective storms, whereas in the C_C cold period rainfall is most commonly the result of regional frontal systems. We acknowledge that this is a simplification, that convective storms can occur in the cold period, and that regional fronts can condition the rainfall regime in the warm period. In the two periods, rainfall events are reconstructed using a different set of parameters. As an example, in a Mediterranean climate, P_2 = 6 hours in the C_W warm period, and P_2 = 12 hours in the C_C cold period (Table 2). When reconstituting a rainfall sub-event, the algorithm checks for the continuity of the rainfall record in the sub-event. If single or multiple "na" measurements (interruptions) are found in the rainfall record in the period covered by the sub-event, the sub-event is excluded from the analysis. If no "na" measurements are found, the sub-event is defined (grey shaded areas in Figure 14c), and rainfall metrics are computed for the sub-event, including: (i) the sub-event duration DS, computed summing the number of hours in the sub-event, and (ii) the sub-event total rainfall E_S, computed by summing the hourly rainfall measurements in the sub-event, $E_S = \sum E_H$.

Step 3: Exclusion of irrelevant rainfall sub-events

Next, the algorithm searches for sub-events that can be considered irrelevant for the reconstruction of rainfall events responsible for landslide occurrence (S_3 in Figure 13). For the purpose, a sub-event is considered irrelevant if the cumulated (total) rainfall for the sub-event is lower than a given threshold value $E_S \leq P_3$, regardless of the duration of the sub-event. In a Mediterranean climate, P_3 = 1 mm (Table 2) is a reasonable threshold to exclude sub-events whose contribution can be considered irrelevant for the possible initiation of rainfall induced

landslides. Irrelevant sub-events (red bars in Figure 14d) are excluded from the subsequent analysis.

Step 4: Identification of rainfall events

In this step, the algorithm aggregates single or multiple sub-events to obtain single rainfall events (S_4 in Figure 13), where a rainfall event is a period of continuous rainfall, or an ensemble of periods of continuous rainfall, separated from the preceding and the successive events by dry periods. Again, the minimum length P_4 of the inter-event dry periods may vary, depending on meteorological and seasonal conditions i.e., $P_4 = P_4(C)$. As an example, to identify the rainfall events shown in Figure 14c, we used a minimum dry period P4 = 48 hours for the C_W warm period, and a minimum dry period of P4 = 96 hours for the C_C cold period (Table 2). Once all the events in the rainfall record are defined (green shaded areas in Figure 14e), the algorithm calculates rainfall metrics for each of the detected rainfall events, including: (i) the event duration D_E, computed summing the number of hours in the rainfall event (including hours for which $E_H = 0$), and (ii) the event total cumulated rainfall E_E, computed by summing the sub-event rainfall $E_E = \sum E_S$.

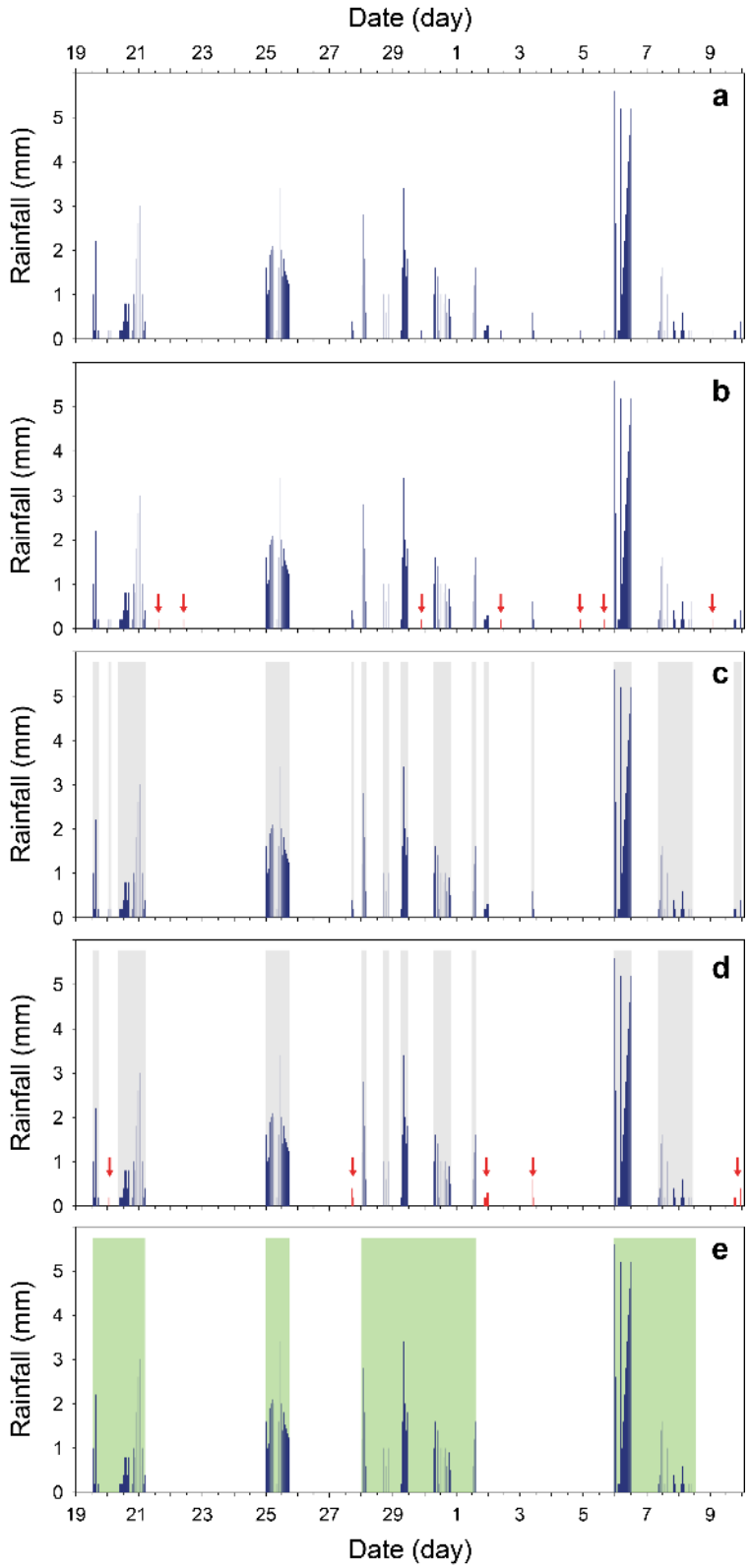

Figure 14. Example of the application of the tool for the reconstruction of rainfall events. (a) Blue bars show hourly rainfall measurements, from 19 September to 10 October 2006. (b) Selection of the isolated hourly rainfall measurements (red bars), shown by red arrows. (c) Identification of the rainfall sub-events, highlighted by grey-shaded areas. (d) Selection of irrelevant sub-events (red bars), shown by red arrows. (e) Identification of rainfall events, highlighted by green-shaded areas.

Table 2. Parameters used by CTRL-T in BLOCK 1. The first column lists the step in the logical framework of the algorithm where the parameter is used (see Figure 13). Two climatic periods are considered: C_W, a "warm" spring-summer period; and C_C, a "cold" autumn-winter period.

Step	Parameter name	Parameter value P(C_W)	Parameter value P(C_C)	Unit
S_0	G_S	2	2	mm
S_1	E_R	2	2	mm
S_1	P_1	3	6	h
S_2	P_2	6	12	h
S_3	P_3	1	1	mm
S_4	P_4	48	96	h

Using the information on the location of rain gauges and landslides provided by the "INPUT" section, "BLOCK 2" picks out the rain gauges closest to each landslide. CTRL-T selects automatically the representative rain gauge for a specific landslide from a pool of rain gauges located in a circular area (buffer) centred on the landslide location and with a parametrized radius (Rb, in Figure 15). Rb depends chiefly on the morphological settings of the study area and on the rain gauge density.

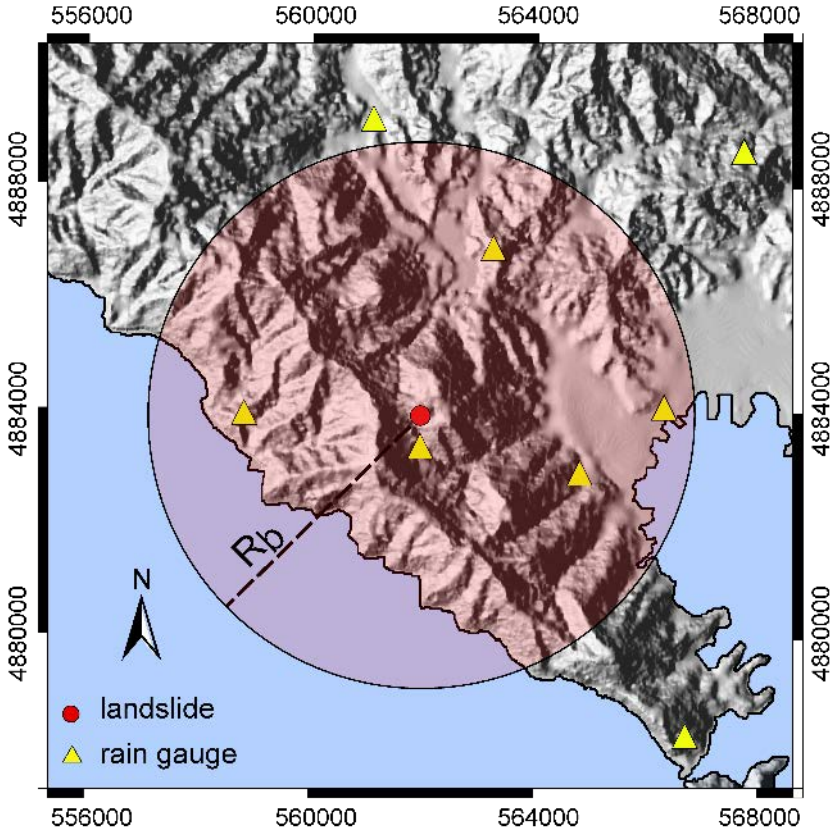

Figure 15. Selection of rain gauges (yellow triangles) in a circular buffer (red shaded area) centred in the landslide location (red dot) with a parametrized radius Rb (dashed black line).

For each selected rain gauge, CTRL-T identifies the rainfall event associated with the landslide. In particular, CTRL-T compares the dates (start date and end date) of the rainfall events identified by “BLOCK 1”, with a record listing the occurrence date (day and time) of the landslides. Each landslide in the temporal record is associated to a single rainfall event (Figure 16a). Next, CTRL-T calculates the rainfall metrics, D_L and E_L, responsible for the slope instability. Note that D_L and E_L responsible for landslide occurrence are not necessarily the same as the rainfall duration D_E and the cumulated event rainfall E_E of the rainfall event in Figure 16a. Most commonly, landslides occur before (and sometimes well before) the end of a rainfall period, and the rainfall after the landslide occurrence cannot be considered relevant for the initiation of the slope failure. In this case, $E_L \leq E_E$ and $D_L \leq D_E$. Occasionally, landslides fail after the end of the rainfall event. In this case, the cumulated rainfall responsible for the landslide corresponds to the cumulated event rainfall, $E_L = E_E$, and the rainfall duration is $D_L = D_E$. For complex rainfall events (Figure 16a) – which are the majority in a typical rainfall record – it is often difficult (or impossible) to decide a single duration, and the corresponding cumulated amount of rain responsible for the landslides. In this case, CTRL-T reconstructs multiple aggregations of rainfall sub-events that are likely to trigger landslides. In Figures 16b, 16c, 16d we show that the complex rainfall event portrayed in Figure 16a is characterized by three sub-events with significantly different rainfall durations (D_L = 28 h, 91 h, and 178 h) and cumulated rainfall amounts (E_L = 104.2 mm, 218.4 mm, and 263.2 mm). Without additional information, the three sub-events identified by the tool are equally probable as possible landslide triggers. Ultimately, CTRL-T identifies a variable number *n* of single (*n* = 1) or multiple rainfall conditions (MRC) likely responsible for each failure (e.g., 3 MRC for the example shown in Figure 15).

Through an empirical relation, that includes the distance between the rain gauge and the landslide, D_L and E_L, a weight *w* is assigned to each pair of the MRC data set.

$$w = \mathrm{f}(\mathrm{d}, E_L, D_L) = d^{-2} {E_L}^2 {D_L}^{-1} \quad (1)$$

The weight is attributed to each (D_L, E_L) pair of the MRC data set. For each landslide, *w* is used to identify the representative rain gauge, and to determine the probability of the single or multiple rainfall conditions to be adopted for the calculation of rainfall thresholds. For a pool of stations enclosed in the radius R_b, the representative rain gauge is the one for which the (D_L,E_L) pair has the highest *w*. In case of multiple pairs, each *w* is normalized to the sum of the individual weights, whereas is set to one in case of a single rainfall condition. The MRC corresponding to the maximum *w* (MPRC) is that likely responsible for the failure (red dot in Figure 16e).

In “BLOCK 3” CTRL-T calculates rainfall thresholds for MRC and MPRC (maximum probability rainfall conditions) data sets, where MPRC is the subset of the (D_L,E_L) pairs with the highest weights (Figure 17).

To define empirical rainfall thresholds and their associated uncertainties, CTRL-T adopts the frequentist statistical method proposed by Brunetti et al. (2010) and modified by Peruccacci et al. (2012) to calculate *ED* thresholds in Italy.

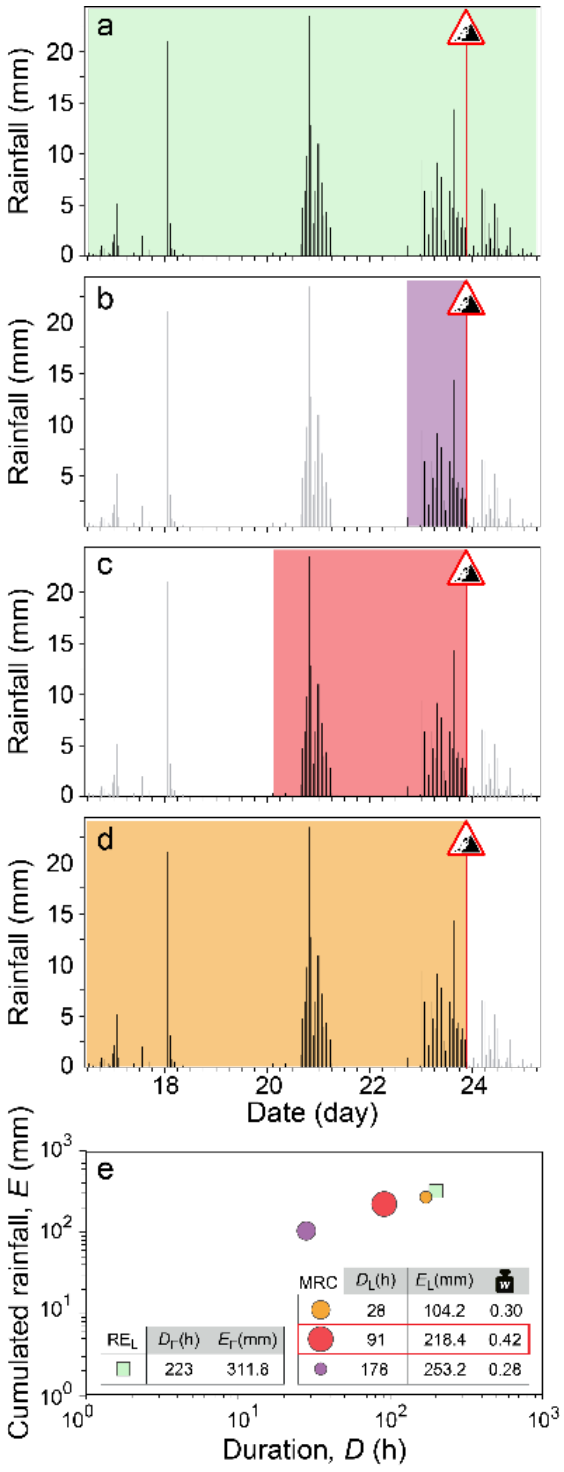

Figure 16. Example of the application of CTRL-T for the reconstruction of the rainfall conditions responsible for a failure. Traffic sign shows time of occurrence (23/12/2006, 10:00 PM), grey bars show hourly rainfall measurements. (a) Rainfall event identified by "BLOCK 1" containing a failure. (b) (c) (d) Multiple aggregations of rainfall sub-events with different values of D_L and E_L. (e). Green square shows the (D_E,E_E) pair of the rainfall event considered in (a). Purple, red, and orange dots show the (D_L,E_L) pairs of the rainfall conditions considered in (b), (c) and (d), respectively. The red rainfall condition is the most likely as trigger of the investigated landslide (MPRC).

The method avoids subjective criteria in the determination of the thresholds, which are common in many of the published rainfall thresholds for the possible initiation of landslides (Guzzetti et al. 2007, 2008). In particular, the method assumes in a Cartesian plane that the threshold curve is a power law of the form:

$$E = (\alpha \pm \Delta\alpha) \times D^{(\gamma \pm \Delta\gamma)} \quad (2)$$

where, E is the cumulated (total) event rainfall (in mm), D is the duration of the rainfall event (in h), α is a scaling parameter (the intercept), γ is the slope of the power law threshold curve, and $\Delta\alpha$ and $\Delta\gamma$ are the uncertainties associated to α and γ, respectively.

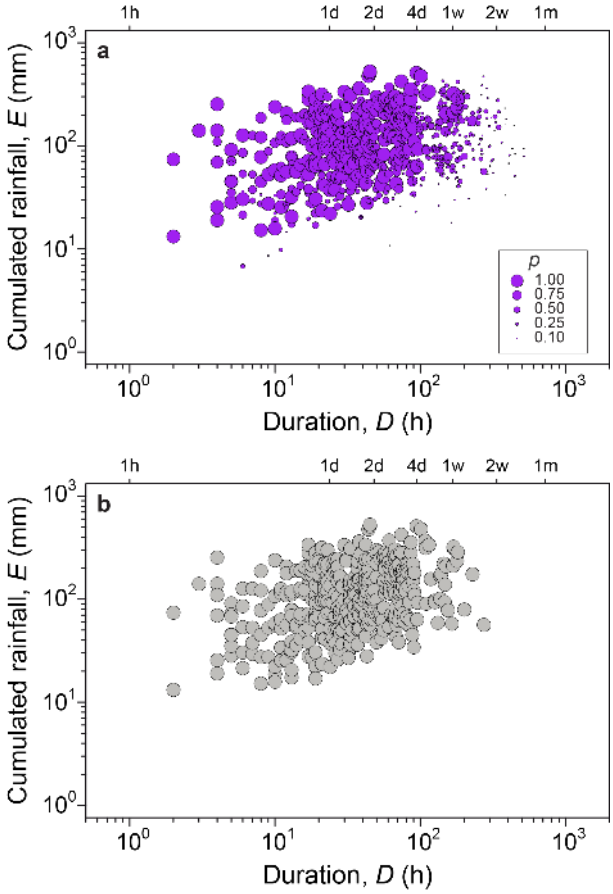

Figure 17. Example of the application of CTRL-T for the reconstruction of the rainfall conditions responsible for failures. Cumulated event rainfall E (mm) vs. rainfall duration D (h) conditions that have resulted in landslides using (a) the MRC and (b) the MPRC data set. In (a) frame, the size of the points (p probability) is proportional to the weight w of the (D_L,E_L) pairs.

Specifically, the ensemble of the (D,E) rainfall conditions responsible for the known slope failures is fitted with a power law. For each event, the difference between the cumulated event rainfall and the fit is calculated. The probability density of the distribution of the differences is determined through a Kernel Density approach, and the result modelled with a Gaussian function. Using the modelled distribution, thresholds corresponding to different non-exceedance probabilities are

calculated (Brunetti et al. 2010). Assuming the set of the empirical (D_L,E_L) points is complete and representative of the conditions that led to slope failures in a study area, the 1% threshold should leave 1% of the rainfall events with landslides below the curve.

A bootstrapping statistical technique is used to determine the uncertainty associated with the parameters α and γ that define the power law threshold curve (Peruccacci et al. 2012). In Eq. (2), α and γ are the mean values of the parameters resulting from the calculation of thresholds for 5000 synthetic series generated by the tool. $\Delta\alpha$ and $\Delta\gamma$ are the standard deviation of α and γ, respectively. Each synthetic series contains the same number n of landslides as the original data set but selected randomly with replacement (bootstrap technique). To calculate the thresholds, a single (D_L,E_L) pair is associated to each landslide. For each landslide in the individual synthetic series, the algorithm samples randomly − with a probability *w* − a single rainfall condition from the MRC data set. The extracted (D_L,E_L) pairs of the n landslide are used to define the thresholds. The algorithm also uses the rainfall conditions with the maximum w to define thresholds for the MPRC data set. The output of the bootstrapping technique consists of 5000 synthetic series of m (D_L,E_L) pairs. Analysis of the *m* synthetic series allows calculating the mean value and the uncertainty associated with the threshold parameters (α and γ) and their respective uncertainties ($\Delta\alpha$ and $\Delta\gamma$). The uncertainties associated with the model parameters decrease as the number of events increases and is also depending on the scatter of the (*D,E*) rainfall conditions around the fit. Figure 18 shows an example of *ED* power law thresholds (T_1, T_5, T_{10}, T_{20}, T_{35}, and T_{50}) corresponding to different non-exceedance probabilities (1%, 5%, 10%, 20%, 35% and 50%, respectively).

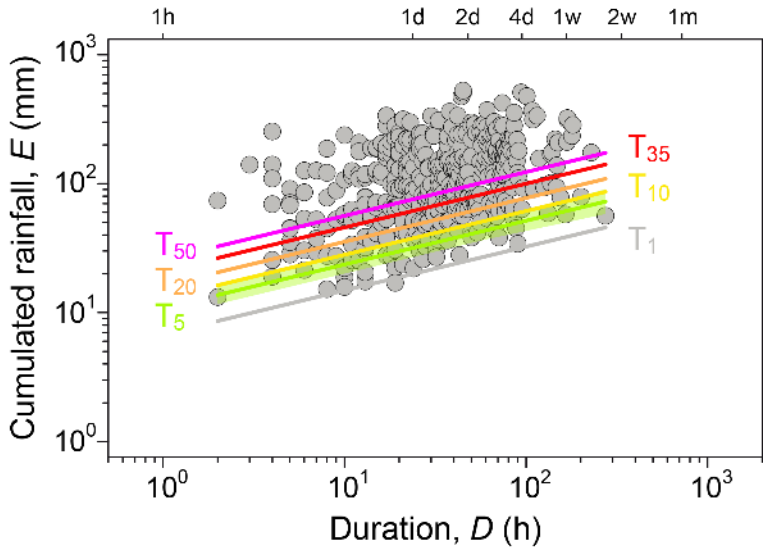

Figure 18. Example of ED rainfall thresholds at non-exceeding probabilities from 1% (T_1) to 50% (T_{50}) for the MPRC data set. Light grey dots are the (D_L,E_L) pairs. An example of the effect of the threshold uncertainty is shown for T_5 (light green shaded area).

Use of the algorithm accelerates greatly the compilation of large catalogues of rainfall events with landslides and reduces the uncertainty in the definition of landslide-triggering rainfall events.

5 RAINFALL THRESHOLDS

Using the catalogues of rainfall events with rock falls presented before, and adopting the tool proposed by Melillo et al. (2018) we determined cumulated event rainfall–rainfall duration (*ED*) thresholds, and their associated uncertainties, for the Gran Canaria and Tenerife test sites. Table 3 lists the number of MPRC used to define the thresholds, the equations of the power law curves used to represent each threshold, with their associated uncertainty, and the range of validity for the thresholds, expressed in hours or days.

Table 3. Rainfall ED thresholds at different non-exceedance probabilities (1%, 5%, 10%, 20%, 35% and 50%) for the Gran Canaria e Tenerife test sites. Note that D must be expressed in days in the equations for the thresholds calculated with daily data, and in hours in the equations for the thresholds calculated with hourly data.

Threshold name	Number of rainfall conditions	Threshold equation	Duration range
$T_{1,Can\text{-}d}$	53	$E = (8.3\pm1.0)\times D^{(0.62\pm0.10)}$	1-11 days
$T_{5,Can\text{-}d}$		$E = (12.3\pm1.2)\times D^{(0.62\pm0.10)}$	
$T_{10,Can\text{-}d}$		$E = (15.1\pm1.4)\times D^{(0.62\pm0.10)}$	
$T_{20,Can\text{-}d}$		$E = (19.5\pm1.8)\times D^{(0.62\pm0.10)}$	
$T_{35,Can\text{-}d}$		$E = (25.5\pm2.5)\times D^{(0.62\pm0.10)}$	
$T_{50,Can\text{-}d}$		$E = (31.9\pm3.6)\times D^{(0.62\pm0.10)}$	
$T_{1,Ten\text{-}d}$	245	$E = (11.6\pm0.6)\times D^{(0.75\pm0.05)}$	1-15 days
$T_{5,Ten\text{-}d}$		$E = (16.3\pm0.8)\times D^{(0.75\pm0.05)}$	
$T_{10,Ten\text{-}d}$		$E = (19.6\pm0.8)\times D^{(0.75\pm0.05)}$	
$T_{20,Ten\text{-}d}$		$E = (24.4\pm1.0)\times D^{(0.75\pm0.05)}$	
$T_{35,Ten\text{-}d}$		$E = (30.6\pm1.4)\times D^{(0.75\pm0.05)}$	
$T_{50,Ten\text{-}d}$		$E = (37.1\pm1.8)\times D^{(0.75\pm0.05)}$	
$T_{1,Ten\text{-}h}$	381	$E = (2.8\pm0.3)\times D^{(0.48\pm0.02)}$	2-712 hours
$T_{5,Ten\text{-}h}$		$E = (4.3\pm0.4)\times D^{(0.48\pm0.02)}$	
$T_{10,Ten\text{-}h}$		$E = (5.3\pm0.5)\times D^{(0.48\pm0.02)}$	
$T_{20,Ten\text{-}h}$		$E = (6.9\pm0.6)\times D^{(0.48\pm0.02)}$	
$T_{35,Ten\text{-}h}$		$E = (9.1\pm0.7)\times D^{(0.48\pm0.02)}$	
$T_{50,Ten\text{-}h}$		$E = (11.4\pm1.0)\times D^{(0.48\pm0.02)}$	

Figure 19 shows, in logarithmic coordinates, the distribution of the (*D*,*E*) rainfall conditions, reconstructed with daily data, that have caused landslides in Gran Canaria (53 blue dots). In the log-log plot, the blue curves are the 1% and 5% *ED* thresholds for the Gran Canaria test site ($T_{1,Can\text{-}d}$, $T_{5,Can\text{-}d}$). In Figure 20, the same thresholds are shown in linear coordinates and in the range $1 \leq D \leq 7$ days, a typical range of rainfall duration used to forecast rainfall-induced landslides. The uncertainties associated with the thresholds (blue shaded areas in Figure 20) are large due to the limited number of (*D,E*) rainfall conditions.

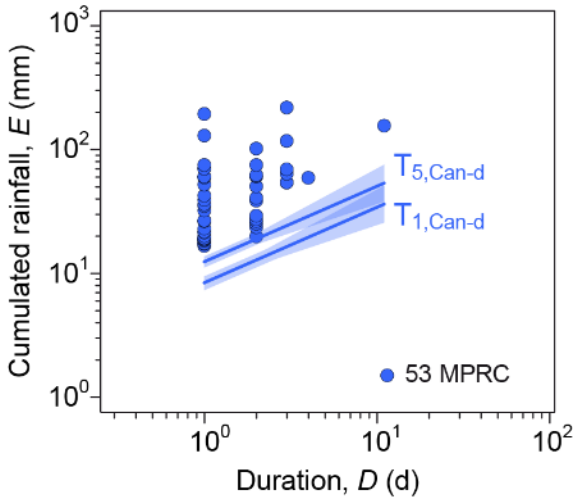

Figure 19. Rainfall duration D (x-axis, in days) and cumulated event rainfall E (y-axis, in mm) conditions that have produced landslides in Gran Canaria test site (53 blue dots). Blue curves are the 1% and 5% power law thresholds ($T_{1,Can-d}$, $T_{5,Can-d}$). Shaded area show uncertainty associated with the threshold curve.

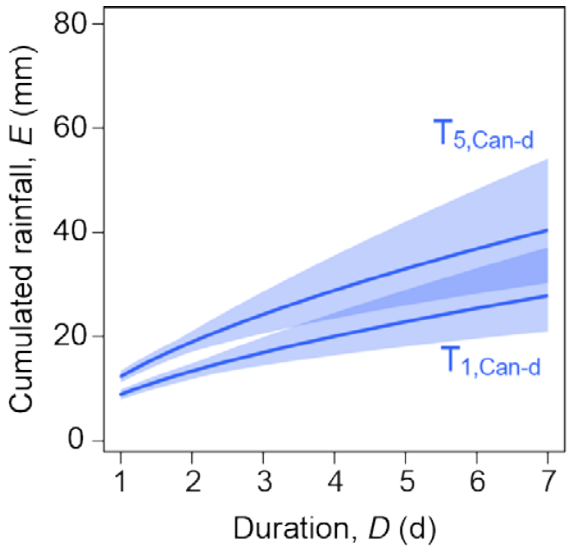

Figure 20. 1% and 5% ED thresholds for Gran Canaria test site ($T_{1,Can-d}$, $T_{5,Can-d}$) in linear coordinates, in the range of durations 1 ≤ D ≤ 7 days. Shaded areas show the uncertainty associated with the threshold curves.

Figure 21 shows, in logarithmic coordinates, the distribution of the (*D*,*E*) rainfall conditions, reconstructed using hourly data, that have caused landslide in Gran Canaria test site (29 orange dots). In the log-log plot, the blue dashed curve is the trend line (fit) of the points. The small number of conditions, precluded the calculation of the thresholds.

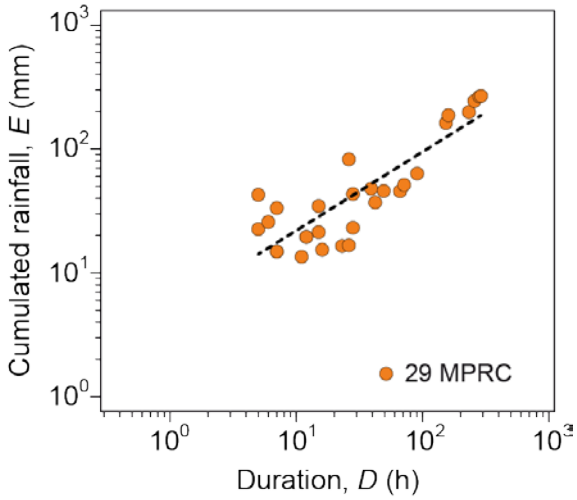

Figure 21. Rainfall duration D (x-axis, in hours) and cumulated event rainfall E (y-axis, in mm) conditions that have produced landslides in Gran Canaria test site (29 orange dots). Dashed curve is the best fit.

Figure 22 shows, in logarithmic coordinates, the distribution of the (*D*,*E*) rainfall conditions, reconstructed with daily data, that have caused landslides in Tenerife test site (245 green dots). In the log-log plot, the green curves are the 1% and 5% *ED* thresholds for the Tenerife test site ($T_{1,Ten\text{-}d}$, $T_{5,Ten\text{-}d}$). In Figure 23, the same thresholds are shown in linear coordinates and in the range $1 \leq D \leq 7$ days.

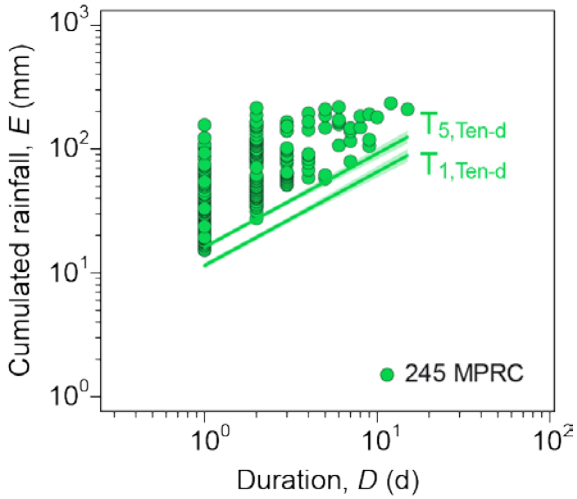

Figure 22. Rainfall duration D (x-axis, in days) and cumulated event rainfall E (y-axis, in mm) conditions that have produced landslides ion Tenerife test site (245 green dots). Green curves are the 1% and 5% power law thresholds ($T_{1,Ten\text{-}d}$, $T_{5,Ten\text{-}d}$). Shaded areas show uncertainty associated with the threshold curves.

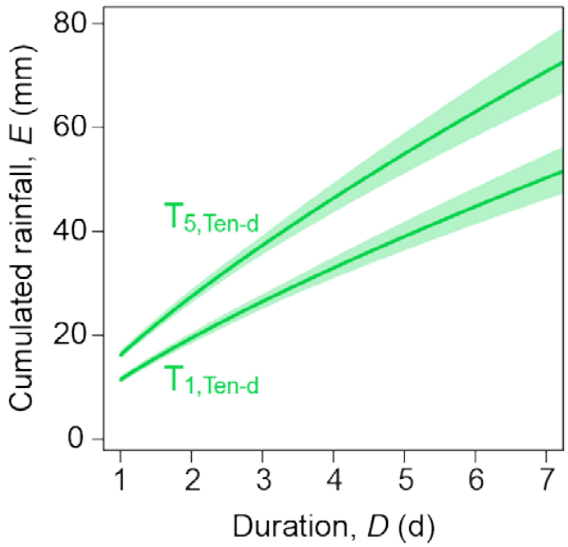

Figure 23. 1% and 5% ED thresholds for Tenerife test site ($T_{1,Ten-d}$, $T_{5,Ten-d}$) in linear coordinates, in the range of durations 1 ≤ D ≤ 7 days. Shaded areas show the uncertainty associated with the threshold curves.

Figure 24 shows, in logarithmic coordinates, the distribution of the (*D*,*E*) rainfall conditions, reconstructed with hourly data, that have caused landslides in Tenerife test site (381 purple dots). In the log-log plot, the purple curves are the 1% and 5% *ED* hourly thresholds for the Tenerife test site ($T_{1,Ten-h}$, $T_{5,Ten-h}$). In Figure 25, the same thresholds are shown in linear coordinates and in the range 1 ≤ *D* ≤ 120 hours, a typical range of rainfall duration used to forecast rainfall-induced landslides.

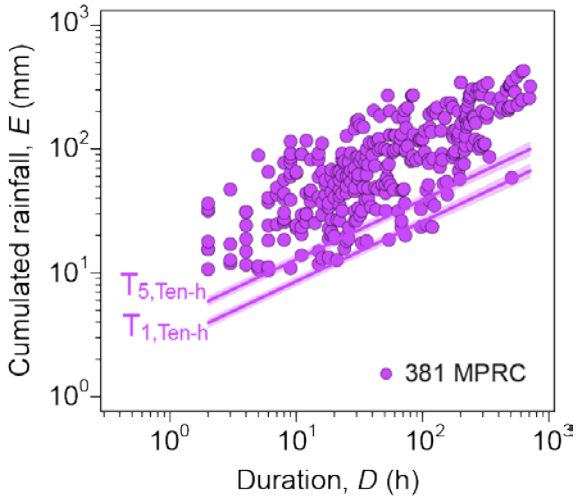

Figure 24. Rainfall duration D (x-axis, in days) and cumulated event rainfall E (y-axis, in mm) conditions that have produced landslides ion Tenerife test site (245 purple dots). Purple curves are the 1% and 5% power law thresholds ($T_{1,Ten-h}$, $T_{5,Ten-h}$). Shaded areas show uncertainty associated with the threshold curves.

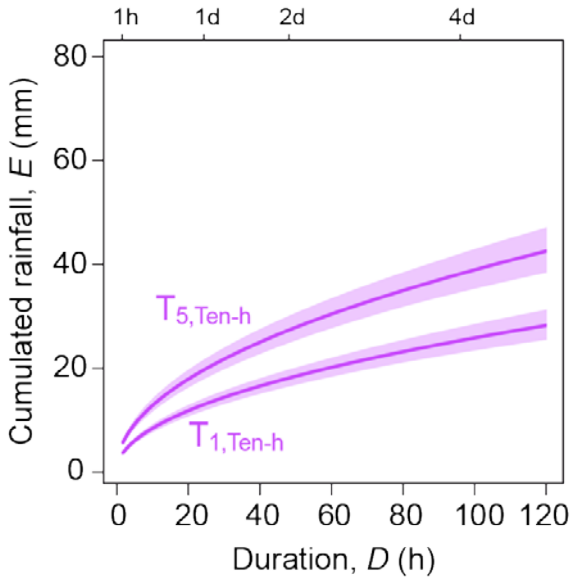

Figure 25. 1% and 5% ED hourly thresholds for Tenerife test site ($T_{1,Ten-h}$, $T_{5,Ten-h}$) in linear coordinates, in the range of durations 1 ≤ D ≤ 120 hours. Shaded areas show the uncertainty associated with the threshold curves.

Figure 26 portrays $T_{5,Ten-d}$ (green curve) and $T_{5,Ten-h}$ (purple curve) in logarithmic coordinates, with the shaded area showing the uncertainty associated with the thresholds. The same thresholds are reported in linear coordinates in Figure 27. Inspection of the figures reveals that $T_{5,Ten-d}$ is steeper and has a duration range shorter than $T_{5,Ten-h}$. The latter, give then limited uncertainty range, has a higher reliability and can be implemented in an operative system for the prediction of rainfall induced rock falls in the test site.

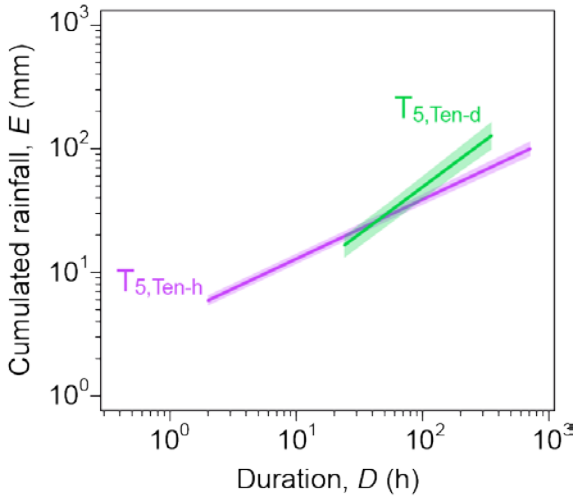

Figure 26. 5% ED thresholds for Tenerife test site defined used daily and hourly rainfall data ($T_{5,Ten-d}$, $T_{5,Ten-h}$) in logarithmic coordinates. Shaded areas show the uncertainty associated with the threshold curves.

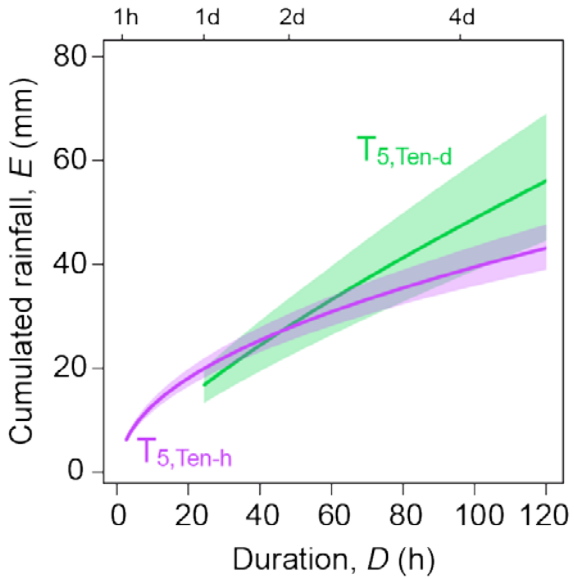

Figure 27. 5% ED thresholds for Tenerife test site defined used daily and hourly rainfall data ($T_{5,Ten-d}$, $T_{5,Ten-h}$) in logarithmic coordinates, in the range of durations 1 ≤ D ≤ 120 hours. Shaded areas show the uncertainty associated with the threshold curves.

Figure 28 portrays the *ED* power law rainfall thresholds ($T_{1,Ten-h}$, $T_{5,Ten-h}$, $T_{10,Ten-h}$, $T_{20,Ten-h}$, $T_{35,Ten-h}$, and $T_{50,Ten-h}$) corresponding to different non-exceedance probabilities (1%, 5%, 20%, 35% and 50%, respectively) for Tenerife test site obtained using hourly data. The equations are reported in Table 3. These thresholds could be used for operative landslide prediction in Tenerife test site.

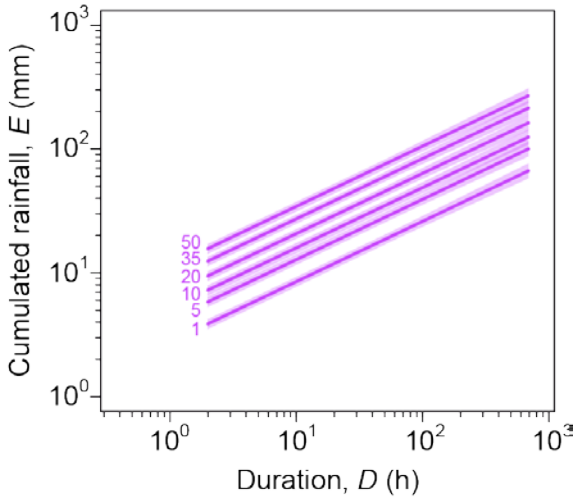

Figure 28. ED rainfall thresholds at 1%, 5%, 10%, 20%, 35% and 50% non-exceeding probabilities ($T_{1,Ten-h}$, $T_{5,Ten-h}$, $T_{10,Ten-h}$, $T_{20,Ten-h}$, $T_{35,Ten-h}$ and $T_{50,Ten-h}$) for Tenerife test site calculated using hourly data. Data shown in logarithmic coordinates.

Figure 29 portrays $T_{5,Can-d}$ (blue curve), $T_{5,Ten-d}$ (green curve), and $T_{5,Ten-d-old}$ (grey dashed curve) in logarithmic coordinates, with the shaded area showing the uncertainty associated with the thresholds. $T_{5,Ten-d\_old}$ is the threshold defined for Tenerife test site in the previous release of the report, with a few number of points. Inspection of the figure reveals that $T_{5,Ten-d}$ and $T_{5,Ten-d\_old}$ are

very similar, almost completely overlapping. On the other hand, $T_{5,CAN}$ and $T_{5,TEN}$ are less similar: $T_{5,TEN}$ is higher and slightly steeper than $T_{5,CAN}$. This could mean that, increasing rainfall duration, a smaller amount of rainfall is necessary to trigger landslides in the Gran Canaria test site, rather than in the Tenerife test site. Moreover, the thresholds defined for the Tenerife test site have uncertainty regions smaller than the thresholds for Gran Canaria test site, because of the larger number of MPRC and the distributions of the MPRC in the *ED* plane.

The trend for the Tenerife test site is confirmed by the new events and the new rainfall measurements used in the present report. On the other hand, the trend for the Gran Canaria test site has to be confirmed by collecting a larger number of events. In the latter case, a larger number of rain gauges with hourly measurements would be necessary for increasing the number of rainfall conditions responsible for the triggering of rock falls and, therefore, for allowing the calculation of reliable hourly rainfall thresholds.

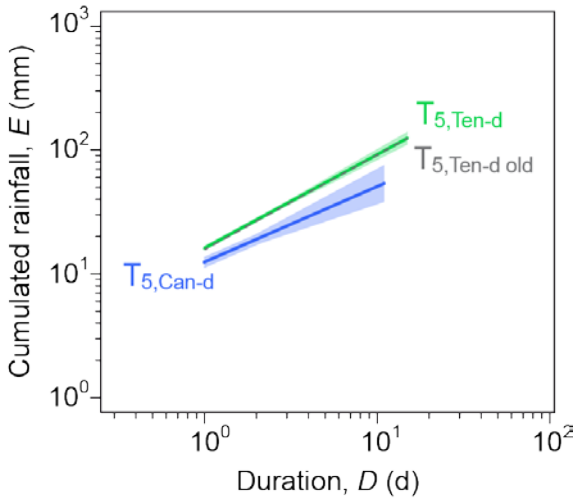

Figure 29. Comparison between the 5% ED thresholds for Gran Canaria ($T_{5,Can-d}$) and for Tenerife ($T_{5,Ten-d}$, $T_{5,Ten-d\_old}$) test sites. Data shown in logarithmic coordinates.

The thresholds for different non-exceedance probabilities obtained for Tenerife test site using hourly rainfall data (Figure 28) are suited for the design of probabilistic schemes for the prediction of rainfall-induced landslides in early warning systems. An improvement in the number of rain gauges providing hourly measurements, as well as in the number of recorded rock falls, would be necessary in Gran Canaria test site in order to allow for the definition of reliable thresholds to be used for the operative prediction of rainfall induces rock falls.

REFERENCES

Aleotti P (2004). A warning system for rainfall-induced shallow failures. Eng. Geol. 73, 247–265. https://doi.org/10.1016/j.enggeo.2004.01.007.

Berti M, Martina MLV, Franceschini S, Pignone S, Simoni A, Pizziolo M (2012). Probabilistic rainfall thresholds for landslide occurrence using a Bayesian approach. J. Geophys. Res. 117, F04006, https://doi.org/10.1029/2012JF002367.

Brunetti MT, Peruccacci S, Rossi M, Luciani S, Valigi D, Guzzetti F (2010). Rainfall thresholds for the possible occurrence of landslides in Italy. Nat Hazards Earth Syst Sci 10, 447–458. https://doi.org/10.5194/nhess-10-447-2010

Campbell RH (1975). Soil slips, debris flows, and rainstorms in Santa Monica Mountains and vicinity, Southern California. US Geol. Survey, Prof. Paper 851, 55pp. https://pubs.usgs.gov/pp/0851/report.pdf

Giannecchini R, Galanti Y, D'Amato Avanzi G (2012). Critical rainfall thresholds for triggering shallow landslides in the Serchio River Valley (Tuscany, Italy). Nat. Hazards Earth Syst. Sci. 12, 829-842. https://doi.org/10.5194/nhess-12-829-2012.

Guzzetti F, Peruccacci S, Rossi M, Stark CP (2007). Rainfall thresholds for the initiation of landslides in central and southern Europe. Meteorol. Atmos. Phys. 98 (3), 239–267. https://doi.org/10.1007/s00703-007-0262-7.

Guzzetti F, Peruccacci S, Rossi M, Stark CP (2008). The rainfall intensity–duration control of shallow landslides and debris flows: an update. Landslides 5 (1), 3–17. https://doi.org/10.1007/s10346-007-0112-1.

Martelloni G, Segoni S, Fanti R, Catani F (2012). Rainfall thresholds for the forecasting of landslide occurrence at regional scale. Landslides 9, 485-495. https://doi.org/10.1007/s10346-011-0308-2.

Melillo M, Brunetti MT, Peruccacci S, Gariano SL, Roccati A, Guzzetti F (2018). A tool for the automatic calculation of rainfall thresholds for landslide occurrence. Environmental Modelling & Software, 105, 230-243. https://doi.org/10.1016/j.envsoft.2018.03.024

Peruccacci S, Brunetti MT, Luciani S, Vennari C, Guzzetti F (2012). Lithological and seasonal control of rainfall thresholds for the possible initiation of landslides in central Italy. Geomorphology, 139-140, 79–90. https://doi.org/10.1016/j.geomorph.2011.10.005.

Peruccacci S, Brunetti MT, Gariano SL, Melillo M, Rossi M, Guzzetti F (2017). Rainfall thresholds for possible landslide occurrence in Italy. Geomorphology, 290, 39–57. https://doi.org/10.1016/j.geomorph.2017.03.031.

Rosi A, Peternel T, Jemec-Auflič M, Komac M, Segoni S, Casagli N (2016). Rainfall thresholds for rainfall-induced landslides in Slovenia. Landslides 13, 1571–1577. https://doi.org/10.1007/s10346-016-0733-3.

Segoni S, Rossi G, Rosi A, Catani F (2014). Landslides triggered by rainfall: a semi-automated procedure to define consistent intensity–duration thresholds. Comput. Geosci., 63, 123-131, 10.1016/j.cageo.2013.10.009.
https://www.sciencedirect.com/science/article/pii/S0098300413002732?via%3Dihub

Staley DM, Kean JW, Cannon SH, Schmidt KM, Laber JL (2013). Objective definition of rainfall intensity–duration thresholds for the initiation of post-fire debris flows in southern California. Landslides 10, 547-562. https://doi.org/10.1007/s10346-012-0341-9.

Wieczorek GF (1996) Landslide triggering mechanisms. In: Landslides: Investigation and Mitigation (Turner AK, Schuster RL, eds). Washington DC: Transportation Research Board, National Research Council, Special Report, 76–90.

Wilson RC (1989) Rainstorms, pore pressures, and debris flows: a theoretical framework. In: Landslides in a semi-arid environment (Morton DM, Sadler PM, eds). California: Publications of the Inland Geological Society, 2: 101–117.